

AD No. 18349

ASTIA FILE COPY

1834

The University of Chicago

Department of Meteorology

ON THE COMPUTATION OF UPPER-LEVEL WINDS FROM  
CONSTANT PRESSURE CHARTS

Prepared Under Contract No. N6ori-02036

Office of Navy Research

August, 1953

# ON THE COMPUTATION OF UPPER-LEVEL WINDS FROM CONSTANT PRESSURE CHARTS

by

L. A. Hughes, E. S. Jordan and R. J. Renard

## Introduction

In the analysis of upper-level charts, the lack of sufficient wind observations remains a significant problem. This deficiency is particularly apparent with the recent aviation requirement of winds at and above the jet stream level and with the advent of forecasting techniques based on a knowledge of the wind field in this region (cf. 1, 9, 12). The present density of wind reports is inadequate to determine the wind field to the degree required for the above and will remain so until it increases to at least that of the raob network regardless of the weather conditions and wind speeds encountered. Until that time, reported winds will have to be supplemented with computed winds in spite of the admitted inadequacies of the latter.

Much has been said in the literature concerning the computation of winds (cf. 3, 5, 6, 8) but little if any has been especially concerned with the high speed winds associated with the jet stream. The purpose of this paper is to introduce and test a computational technique that considers the special problems of upper-level high-speed winds and yet is simple enough to be applied in routine analysis and forecasting.

## Preliminary Considerations

A factor which is generally neglected in the computation of low-speed winds, but which must be considered here, is the choice of a map projection suitable for analysis of the height field. Of the maps most frequently used for mid-latitude analysis, the polar stereographic and the Lambert conformal conic, only the latter is suitable. The reason being that only on this projection will the curvature of a line on the map closely approximate the geodesic curvature of the line on the earth except for scale differences. When using the stereographic projection, the difference between the real and the measured curvature can result in errors of 20-25 per cent in the computed wind in the jet stream region, for the error is directly proportional to the wind speed as well as inversely proportional to the latitude (when south of the true parallel, and the curvature.

A painstaking analysis of the height field at the level of interest is assumed in the discussion since computed wind speeds are, of course, primarily dependent on the height gradient. The reader is referred to (1) for a detailed discussion of the problems involved in such an analysis.

Neiburger et al (5) found that for winds at the 700-mb level, computations using the geostrophic assumption gave just as good results as those using the gradient assumption. But this result would not be expected at upper levels where the wind speeds are much higher, for the gradient correction is a second order function of the wind speed. Therefore, the method of computation to be discussed is based on the gradient wind assumptions.

#### Construction of the Gradient Wind Nomograms

Nomograms were constructed from the gradient wind equation as expressed by

$$\frac{V^2}{R_t} + f(V - V_g) = 0 \quad (1)$$

where  $V$  is the gradient wind,  $V_g$  is the geostrophic wind,  $f$  is the coriolis parameter, and  $R_t$  is the radius of curvature of the trajectory of the air parcel (positive for cyclonic). The parameters of this equation are easily calculated from a constant pressure chart with the exception of  $R_t$ . The usual assumptions in this regard are to consider  $R_t$  equal to the radius of curvature of the streamlines ( $R_s$ ), which in turn is equal to that of the contours ( $R_c$ ).

These assumptions signify the existence of a stationary steady state pattern of contours. However, this is not usually the case in the atmosphere. Considering  $R_s$  equal to  $R_c$  is tantamount to saying that there are no accelerations along the streamlines, i.e., the wind blows parallel to the contours. This assumption is the more justifiable under the circumstances as it is inherent in the gradient wind equation. The error thus introduced would most likely be a minimum in the lower levels of the atmosphere and a maximum in the jet stream. Unfortunately the present data network and computational difficulties void considering accelerations at any level and especially so in the region of the jet stream. We shall, therefore, have to neglect them to keep our computational method simple. Because the sign of the acceleration is not systematic (see 10), the resulting error should not be systematic.

Considering  $R_t$  equal to  $R_s$  implies no movement or change in shape of the contour field. This is not inherent in the gradient wind equation. Use of this assumption would cause the computed winds to be lower than the true gradient wind under cyclonically curved flow and higher under anticyclonically curved flow. Thus a systematic error is produced which should be eliminated if possible.

It has been shown (7) that in a system moving with no change in shape, the relationship between  $R_t$  and  $R_s$  can be expressed by the equation

$$R_s = R_t \frac{V - C \cos \psi}{V} \quad (2)$$

Where  $C$  is the speed of motion of the pressure system and  $\psi$  is the angle between the wind direction and the direction of motion of the pressure system. In the case of the quasi-sinusoidal wave pattern typical of upper-level patterns,  $\psi$  would generally be less than  $45^\circ$  so that  $\cos \psi$  would be larger than 0.7. In the vicinity of the trough and ridge lines, where the gradient correction is largest and errors in curvature more significant, the angle  $\psi$  would generally be much smaller than  $45^\circ$ , since these lines move in a direction almost perpendicular to themselves and are of necessity perpendicular to the contours. In this case the value of  $\cos \psi$  would be very close to 1.0. With good approximation, we therefore obtain the following equation by combining equations (1) and (2):

$$\frac{V^2 - VC}{R_s} + f(V - V_g) = 0 \quad (3)$$

This equation was graphed so that computations could be quickly and easily made. The result is presented in Fig. 1 (cyclonic case) and Fig. 2 (anticyclonic case).<sup>1</sup> The nomograms are for a particular latitude and a particular value of  $C$  with provision for adjustment for other values of these parameters. In the construction a value of 20 knots was used for  $C$  since that is approximately the average value found by Namias (4) at 700 mb, and the speed of pressure systems is known to be approximately constant with height. For computation purposes the value of  $C$  may be determined from the speed of the nearest trough or ridge line.

#### Comparison of Computed and Observed Winds

To test the value of the nomograms and wind computations in general, a number of computed winds were compared with observed winds and the deviations noted. A number of winds were computed from a series of 25 300-mb charts for the first half of November 1951. The regions chosen for the test were those with a maximum of data, namely the United States and Great Britain, with 18 per cent of the winds coming from this latter area. The choice was made with the aim of obtaining a good contour analysis. These analyses were carefully made with the primary concern being to draw for the height data although the wind data was on the chart at the time. A wind was computed for each station that reported a wind at 300 mb provided the radius of curvature of the contour and the geostrophic wind could be measured fairly reliably. This eliminated computations very near centers, in very sharp troughs and ridges, and in regions where the contours began to converge or diverge sharply. This was not a major restriction as very few winds were eliminated for these reasons. Only winds above 25 knots were considered.

The computations were performed using the nomograms described above and the geostrophic assumption in cases of straight flow. They will be considered under three classifications: Cyclonic, anticyclonic, and no-curvature. The definition of this latter group is somewhat indefinite since a curvature correction is not significant beyond a certain point dependent on the wind speed, and these low curvatures can be considered straight flow for practical purposes. For most winds

<sup>1</sup>For the details of the construction and use of the nomograms see the Appendix.

a radius of curvature in excess of  $40^\circ$  latitude can be neglected as having no significant effect on the computation. However, for winds much above 100 knots, as found in the region of the jet stream, this is not true. For example, a gradient wind computed to be 250 knots, using a cyclonic radius of curvature of  $53^\circ$  latitude, would become a 300 knot wind if the curvature correction were neglected--a 20 percent error. Just how large a radius of curvature it is possible to measure with the curve fitting or other methods is open to question. It is doubtful if values as large as  $40^\circ$  latitude can be accurately measured at times, whereas much larger values can be measured when we have a current of considerable length with little curvature change along it. As a compromise, radii of curvature up to  $80^\circ$  latitude were measured whenever possible, with the remaining winds considered as "no curvature" cases. This problem is not significant as far as this comparison is concerned as only two winds larger than 125 knots were observed. It would be much more so in the case of an actual wind analysis since the very high winds are most likely to be missing from the reports and must, therefore, be computed.

The distribution of the winds used in the test is given in Table I.

Table I. Distribution of 468 observed winds (in per cent)

Observed wind speed (knots)	25-49	50-74	75-99	100---	Total
Cyclonic	18	17	8	2	45
Anticyclonic	12	13	4	1	30
No-curvature	10	11	4	0	25
Total	40	41	16	3	100

Of the anticyclonic winds, almost half were in a region which the radius of the contours was smaller than the minimum radius possible with balanced gradient flow (see (2) for discussion of minimum radius). Under such conditions, a gradient computation was not possible. The distribution of these winds with respect to speed was quite similar to that shown in Table I for all anticyclonic winds.

Cyclonic and no-curvature cases. Fig. 4 is a cumulative frequency distribution of the deviations (positive and negative) of the computed from the observed wind speed speed comparing the gradient and geostrophic winds for the cases with cyclonic flow. It can readily be seen that here the gradient speed is a better approximation to the observed speed than the geostrophic. Of course, the observed wind due to its inaccuracies may be different from the real wind so that the deviation of computed winds from real winds could be somewhat different from that given above, but it would not necessarily be so.

Fig. 5 gives the frequency distribution of errors for the cyclonic and no curvature groups with positive deviation indicating a computed wind larger than the observed. The curve for the cyclonic group using the gradient wind (Fig. 5a) is fairly symmetrical with a mode of about zero. It indicates that 30 per cent of the computations came within  $\pm 10$  per cent of the observed wind speed and about 70 per cent within  $\pm 30$  per cent (see also Fig. 4).

The curve for the no-curvature group (Fig. 5b) is quite similar but has a mode slightly greater than zero. This is probably due to the fact that cases with large radii of curvature were considered to have no curvature and that these cases were predominately cyclonic. Thus, if the small curvature correction had been applied, the computed wind would have been slightly lower. Approximately the same accuracy is indicated as in the cyclonic case.

To improve these distributions the large percentage errors should be eliminated. In an attempt to do this, all cases with errors greater than 30 per cent were examined to determine if a common factor existed such that these cases could be eliminated.

Grouping according to the radius of curvature failed to yield the desired factor as the errors were fairly evenly distributed except for a slight tendency for large errors to occur when the radius of curvature was small. The investigation of the effect of wind speed was more fruitful, however. In both cyclonic and no-curvature cases, it was found that most of the large errors occurred with winds less than 50 knots. In Fig. 5 the dashed curves give the distribution of errors for the cases where the actual wind was  $\geq 50$  knots. The fact that large errors occur at low wind speeds could very likely be due to the use of percentages instead of absolute values.

Because of the fairly large amount of dispersion still remaining in the curve of the cyclonic winds, the significance of the correction for movement was investigated. A tabulation of the speed of the trough and ridge lines showed that 90 per cent fell in the range 0-40 knots, while 40 per cent fell within 15-25 knots. When the average speed of movement--20 knots--was assumed for all of the cases there was no appreciable change in the curve as presented in Fig. 5a. This is readily seen from the nomogram as well, for use of the average speed of movement instead of the real speed results in an error of less than 10 per cent in the wind speed for any computation made to the right of the short dashed curve at the far left on the nomogram provided the real speed lies between 0 and 40 knots, inclusive.

Some positive skewness is to be expected in all of the curves due to the use of percentages, for then the size of the deviation is much more restricted on the negative side than on the positive side.

Anticyclonic case: The anticyclonic graph, Fig. 6, shows an entirely different picture from that of the cyclonic graph for now the gradient wind speed is, on the average, no improvement over the geostrophic speed. In fact, the geostrophic is even somewhat better.<sup>2</sup> This is surprising since the curvature correction is more significant under anticyclonic conditions than under cyclonic conditions. The most readily available explanation is concerned with the concept of a minimum radius of curvature. As has been stated, half of the cases selected under anticyclonic conditions had radii of curvature smaller than the minimum and a gradient computation could not be made. Of the remaining winds, most had curvature radii quite near the minimum. This would lead one to the conclusion that, with anticyclonically curved flow in the upper troposphere, non-gradient conditions are the rule rather than the exception.

The anticyclonic case, therefore, presents considerable complication because it is desirable to be able to obtain an estimate of the wind even when a gradient computation is not possible due to a small curvature radius, and also because the gradient wind does not appear to give good results when it can be used. For these reasons, it

---

<sup>2</sup> When those winds for which a gradient computation was not possible are included in the geostrophic curve of this figure, there is no great change.

was decided to see what could be obtained from the geostrophic wind. All the geostrophic winds are included in the following considerations, as it was found that in each of the cases the separate curve for all winds did not differ appreciably from the curve for those cases when a gradient computation was possible.

The winds were first divided into groups with reported speeds of  $< 50$  knots and  $\geq 50$  knots. Fig. 7a is the frequency distribution of errors for those  $< 50$  knots. This curve shows a mode of zero and an accuracy comparable to that shown in the dashed curves of Fig. 5. Fig. 7b is for those winds  $\geq 50$  knots. It has a mode which is definitely negative as would be expected. A shift in this mode so that the curve would be more or less symmetrical around zero can be accomplished by adding 20 per cent to each of the geostrophic winds. The result of such an addition is shown in the dashed curve. This latter method of computing, while strictly empirical, allows an estimate of the wind speed under conditions that would preclude a gradient computation, and yet give an accuracy comparable to the best attained above.

### Analysis of Errors

The question immediately arises as to why, in spite of the care exercised in making the computations, do deviations of 50 per cent or more still occur. The cause must be that the base for comparison was inaccurate, the assumptions in the method were not fulfilled, or the method was not applied correctly. These may be broken down for discussion under the following:

- (1) Inaccurate rawins
- (2)  $R_s \neq R_c$
- (3) Angle  $\psi \neq 0$
- (4) Analysis errors

(1) While rawins are not accurate, they are the best that are available. Their errors can be appreciable upon occasion, however, due to such things as low elevation angles and evaluation by incompletely trained personnel.

(2) Of the non-gradient terms in the equations of motion that have been neglected, the acceleration term is probably the most significant. It will produce cross-contour flow such that  $R_s \neq R_c$ . From a sample of 257 winds in the jet stream region, Riehl and Jenista (10) found that the winds blew across the contours at angles larger than  $30^\circ$  in 20 per cent of the cases and angles larger than  $45^\circ$  occurred in 5 per cent of the cases. Part of their data was taken over the same region and for the same period as the winds considered here. While the measurement of such angles is probably subject to considerable error using the present wind reporting network, some cross-contour flow should exist and, even allowing for some error, the data in (10) show that large angles do occur. Cross-contour flow will cause  $R_s$  to be different from  $R_c$  but the effect on the computed wind speed is difficult to evaluate. While it is possible that the difference in curvature used could cause such large errors by itself, cross-contour flow also signifies a different balance of forces from that



assumed under the gradient wind equation. It is believed, therefore, that cross-contour flow can account for a large portion of the deviations that occurred but that deviations in excess of 50 per cent are probably not due to this factor alone.

(3) The assumption that the wind blows parallel to the direction of motion of the system should be quite good for this and most series of charts at high levels, for you do not have rapidly moving closed centers but have instead smaller wave-like perturbations (short waves) moving along the basic current (the long-wave pattern). The largest deviations from this assumption occur in the vicinity of the inflection point of the flow--a region in which the gradient correction to geostrophic flow will be quite small anyway.

(4) The analyses for this test were made by the authors. Data missing from the regular teletype reports were obtained from the source so that the coverage was as complete as possible. With the present radiosonde network, however, it is impossible to approach a unique analysis. This was well demonstrated when the analyses were examined in regions where large errors were made in computing the winds. In many cases it was possible to change the analysis to greatly reduce the error without disregarding existing data. It is, therefore, believed that errors in the computed wind speed of 50 per cent or more can still originate in analytical errors.

### Conclusions

From the above, it appears that the computation of winds from a pressure field can never give winds of the accuracy needed, due to analytical errors and the non-gradient effects in the atmosphere. Therefore, it seems that the only way to obtain a wind field at upper levels accurate enough for forecasting and navigational purposes is to increase the number and accuracy of observed winds.

At present, we must still make wind computations. Consideration of the above suggests that when computing winds in the region of the jet stream three methods should be used:

(1) Under cyclonic flow conditions use the attached gradient computer and the brief method of computation (using the average  $C$ ). This will produce wind speeds with probable errors of less than 10 per cent one-third of the time, and with errors of less than 30 per cent two-thirds of the time. Better results will be obtained if the computations are restricted to regions where the winds are expected to be greater than 50 knots.

(2) Under "no-curvature" flow, the neglect of radii of curvature beyond  $80^\circ$  latitude has no appreciable effect, and the geostrophic wind will give as good results as the gradient wind does with cyclonic flow. Again if the computations are restricted to places where the winds are expected to be greater than 50 knots the results will be better.

(3) Under anticyclonic flow the geostrophic wind should be used if it is less than 40 knots. If it is greater than this it should be increased by 20 per cent. With this method, results will be obtained comparable to (1) and (2) above.



It should be remembered that the nomograms and other computational techniques suggested above are for use in regions of the jet stream--300 mb to 200 mb. Their use at other levels is questionable. This is so partly because the nomograms were constructed under the assumption that the angle between the wind direction and the movement of the streamline field was quite small. Therefore, at any level in the atmosphere where the flow pattern consists of many closed highs and lows, this assumption will not be generally valid. Another factor is that the method of computing winds under anticyclonic flow conditions is based on a statistic obtained with data at the 300-mb level. It is, therefore, applicable only in that vicinity.

#### Acknowledgements

The writers are indebted to Drs. H. Riehl and N. E. La Seur for their advice and criticism.

## APPENDIX

The nomograms were constructed from equation 3, using a particular latitude ( $43^\circ$ ) and a particular value of the speed of the system (20 knots). The ordinate is the geostrophic wind speed in knots ( $V_g$ ); the abscissa is basically the radius of curvature of the contours (streamlines) in degrees latitude at the point of computation ( $R_g$ ). The gradient wind is obtained from the solid curving lines labeled in knots.

To correct for latitudes other than  $43^\circ$ , multiply  $R_g$  by the factor  $k$ , as obtained from Table I on the nomograms. When the speed of the system does not equal 20 knots use the dashed lines radiating from the lower left corner of the nomogram and Table II on the nomogram to obtain a correction to the gradient wind for  $C = 20$  knots.

A brief method of computation which eliminates estimating and correcting for the speed  $C$  is performed simply by assuming  $C = 20$  knots, the average value. This will cause an error of less than 10 per cent in the computed wind provided the actual speed  $C$  lies within the range 0 to 40 knots and provided the computation is performed in the region of the nomogram to the right of the short dashed curve. This dashed curve is located at the far left on the nomogram.

To obtain the radius of curvature of the contours it is suggested that a tool similar to that of Fig. 3 be used. The values to the left of the curves give the value of  $R_g$  in degrees latitude appropriate to the scale and projection of the map used; the values on the right give  $kR_g$ . To use this it should be transparent so that it can be placed over a map and the curve of the contours matched with one of the curves on the overlay.

REFERENCES

- (1) Alaka, M. A., C. L. Jordan, and R. J. Renard, 1953: The Jet Stream. University of Chicago, NAVAER 50-IR-249, 85 pps.
- (2) Bjerknes, J., 1951: Extratropical Cyclones, Compendium of Meteorology. Boston, Amer. Meteor. Soc., pp. 577-598.
- (3) Godson, W. L., 1948: A New Gradient Wind Nomogram, Bull. Amer. Meteor. Soc., #29, pp. 95-100.
- (4) Namias, J., 1947: Extended Forecasting by Mean Circulation Methods. Washington, D. C., U. S. Department of Commerce, 89 pps.
- (5) Neiburger, M., et al, 1948: On the Computation of Wind from Pressure Data, J. Meteor., #5, pp. 87-92.
- (6) Petterssen, S., 1940: Weather Analysis and Forecasting. New York, McGraw-Hill, pp. 224-225.
- (7) \_\_\_\_\_, 1945: Computation of Winds in the Free Atmosphere. Washington, D. C., NAVAER 50-IR-166, 13 pps.
- (8) Rex, D. F., and H. V. Church, 1944: A Gradient Wind Nomogram for Use with the Surface Chart, Bull. Amer. Meteor. Soc., #25, pp. 414-419.
- (9) Riehl, H., and C. O. Jenista, 1952: A Quantitative Method for the 24-Hour Jet Stream Prognosis, J. Meteor., #9, pp. 159-166.
- (10) \_\_\_\_\_, et al, 1952: Forecasting in Middle Latitudes, Monograph #5. Boston, Amer. Meteor. Soc., 80 pps.
- (11) University of Chicago, Department of Meteorology, 1952: Experiments in Quantitative Prediction with the Aid of Upper-Air Charts, edited by L. A. Hughes, A Technical Report to the Office of Naval Research (mimeographed).

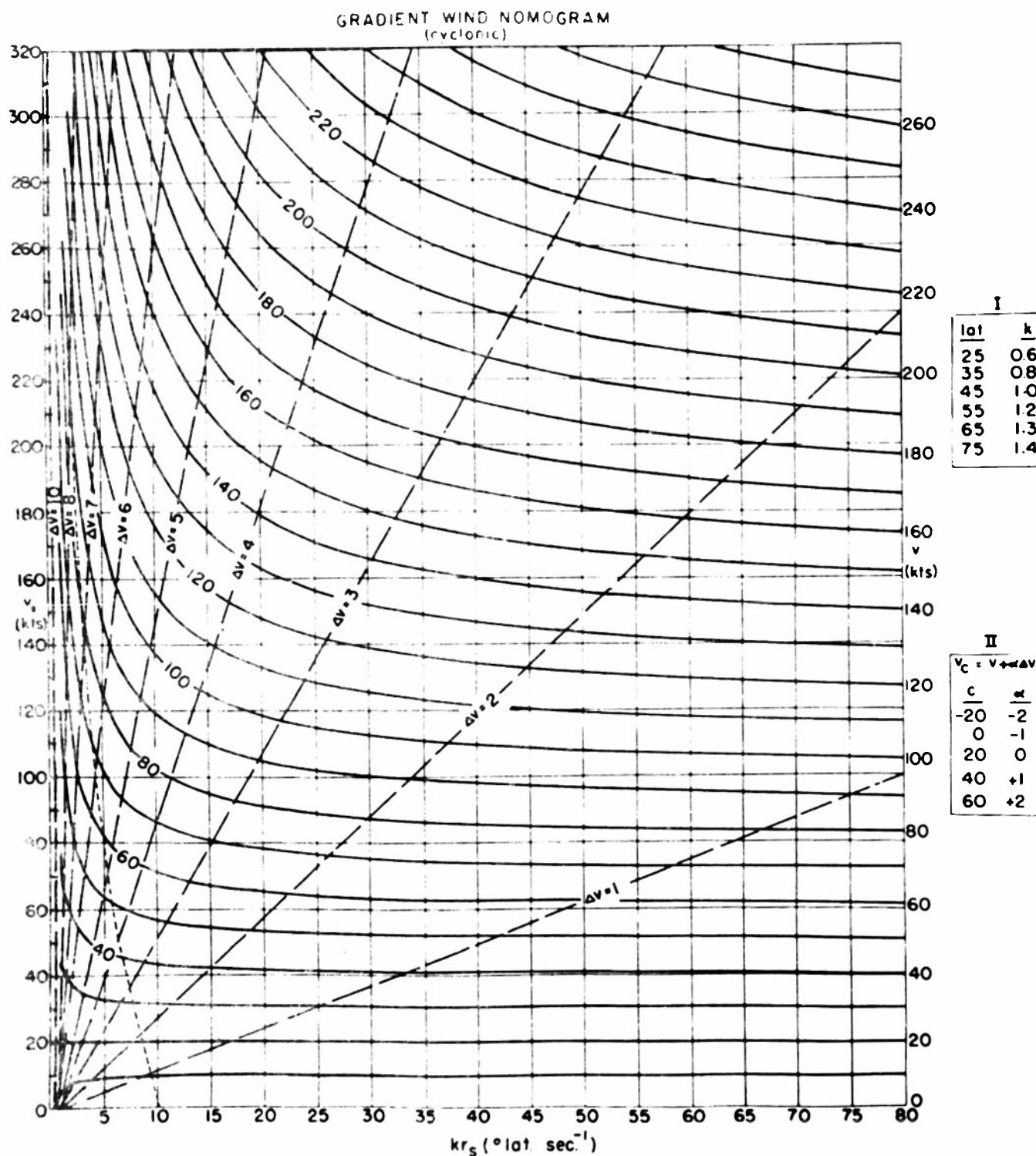


Fig. 1: Gradient wind nomogram for cyclonic curvature.

- (1) Determine  $kR_s$  using Table I and the radius of curvature of the contour (streamline).
- (2) Enter graph with this value ( $kR_s$ ) and the geostrophic wind ( $V_g$ ). At their intersection obtain value for gradient wind ( $V$ ).
- (3) Using speed of system along streamlines ( $C$ ) correct  $V$  according to Table II, obtaining  $V_0$ . Brief Method: Eliminate step No. 3-- this introduces error  $< 10\%$  in area to right of short-dashed curve, assuming  $0 \leq C \leq 40$  kts.

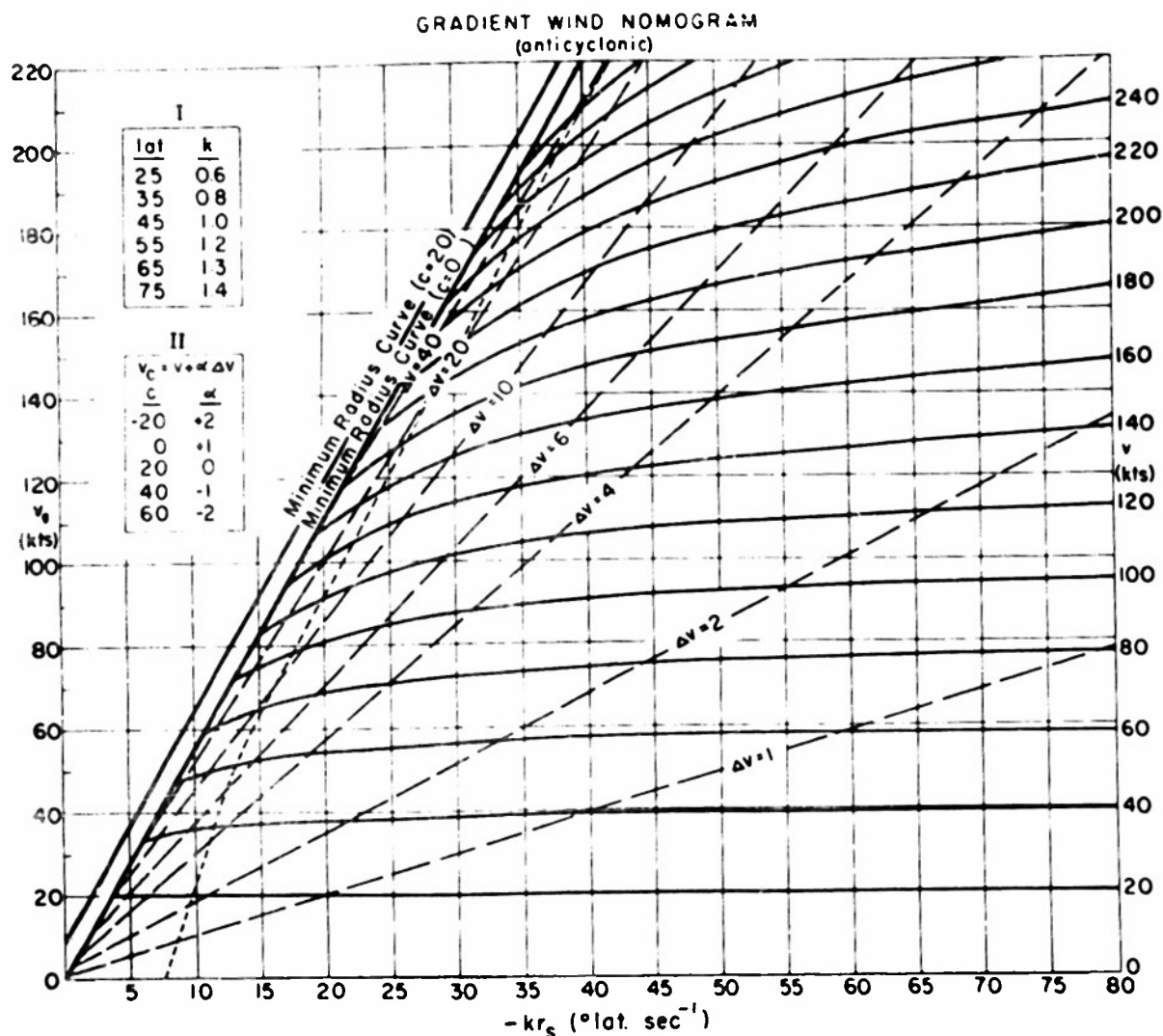


Fig. 2: Same as Fig. 1 for anticyclonic curvature

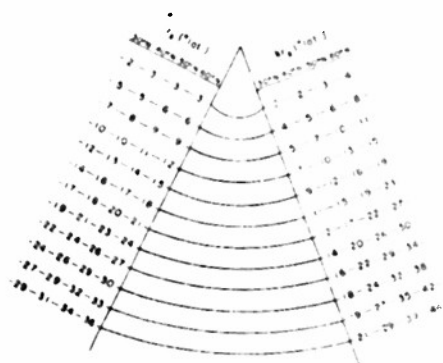


Fig. 3:

An example of an overlay for obtaining radius of curvature. The values of  $R_g$  given on the left of the overlay are radii of curvature corrected only for the latitude of the computation point. The values on the right are multiplied by the appropriate  $k$  as given in Table I on the gradient wind nomograms (Fig. 2).

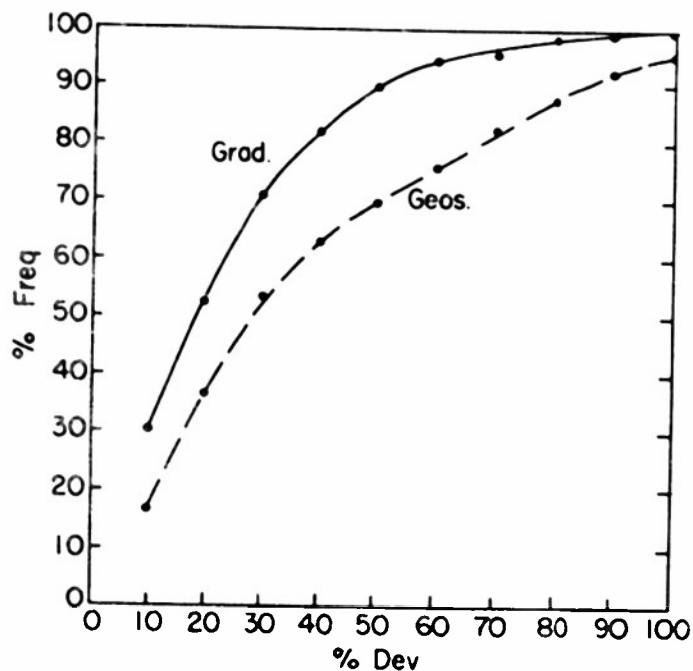
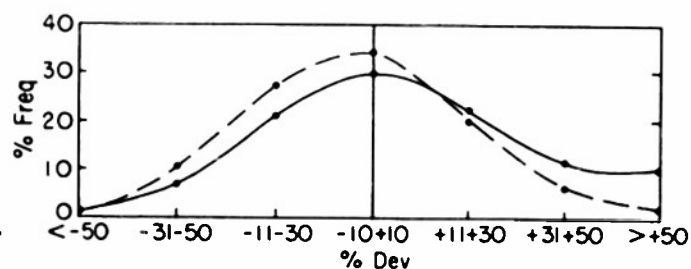


Fig. 4:

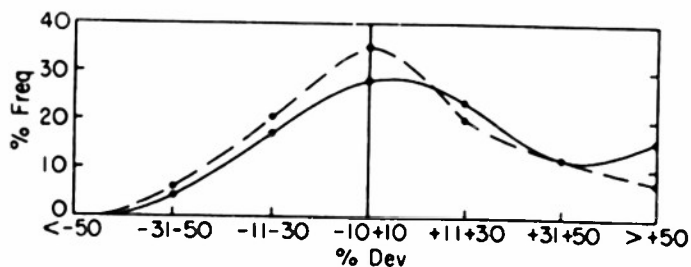
Cumulative frequency curves for cyclonic winds. The solid curve is the per cent deviation of the gradient from the observed winds. The dashed curve is the per cent deviation of the geostrophic from the observed winds.

Fig. 5:

Frequency distributions of the per cent deviation of the computed wind from the observed wind, with positive values indicating a computed wind larger than the observed wind.



a. Cyclonic winds. The solid curve gives the distribution of errors of all the gradient winds. The dashed curve includes only observed winds  $\geq 50$  knots.



b. No curvature. The solid curve gives the distribution of errors of all the geostrophic winds. The dashed curve includes only observed winds  $\geq 50$  knots.

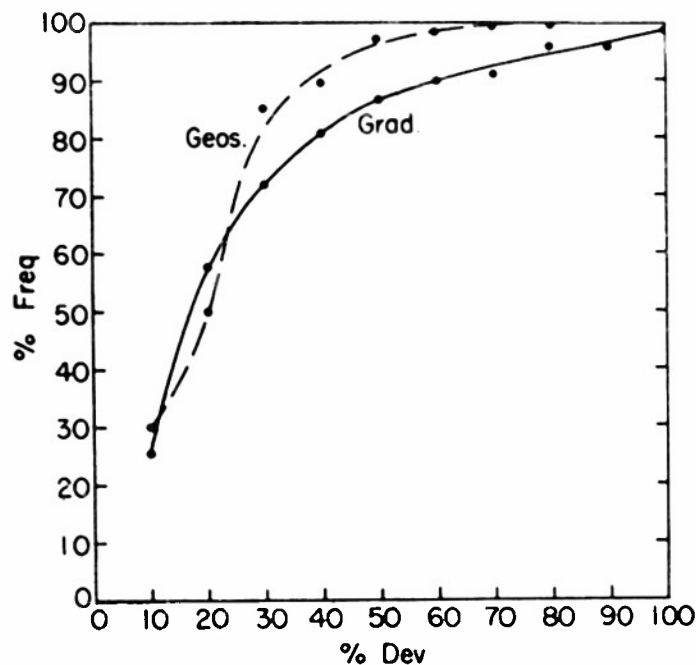
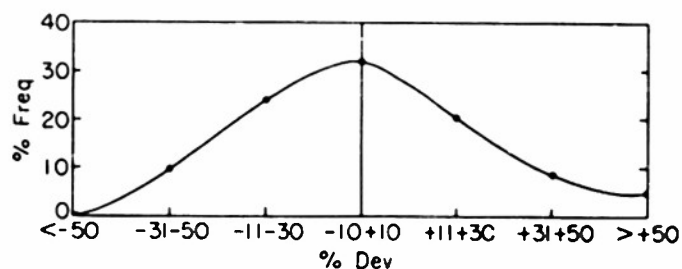
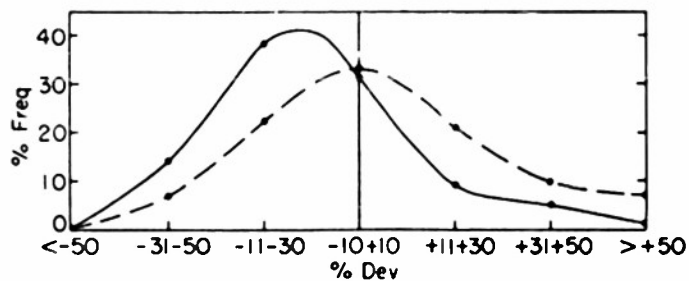


Fig. 6: Same as Fig. 4 for anticyclonic winds.

Fig. 7  
Same as Fig. 5  
for anticyclonic  
winds.



a. The distribution of errors of the geostrophic wind includes only those observed winds  $< 50$  knots.



b. The solid curve is the distribution of errors of the geostrophic wind for observed winds  $\geq 50$  knots. The dashed curve is the distribution of errors of the geostrophic wind plus 20 per cent.